

Numerical solution for heat transfer of Oldroyd-B fluid over a stretching sheet using successive linearization method



Faisal Salah *

¹Department of Mathematics, College of Science and Arts, King Abdul-Aziz University, Rabigh, Saudi Arabia²Department of Mathematics, Faculty of Science, University of Kordofan, Elbid, Sudan

ARTICLE INFO

Article history:

Received 12 October 2019

Received in revised form

8 March 2020

Accepted 10 March 2020

Keywords:

Oldroyd-B fluid

Successive linearization

Stretching sheet channel

ABSTRACT

The objective of this study is to find the numerical solution for the MHD flow of heat transfer to the incompressible Oldroyd-B liquid on a stretching sheet channel. The partial differential equations governing this system are converted into ordinary differential equations using similarity conversion. The resulting nonlinear equations governing the flow problem are numerically solved by the successive line method (SLM). Numerical results are derived and presented in tables for some comparisons. These comparisons are important in demonstrating the high accuracy of SLM in solving the system of nonlinear differential equations. These solutions take into account the behavior of Newtonian and non-Newtonian fluids. It is reported that Deborah number in terms of relaxation time resists and slows down the motion of fluid particles at various time instants. Temperature profile increase by increasing Deborah number in terms of relaxation time. The graphical results of various non-Newtonian parameters such as coefficient of mixed convection, Hartman, Deborah, and Prandtl number on the flow, field, and analysis are also discussed. In addition, the current results were tested and compared to the published results available in a limited manner, and an excellent agreement was reached.

© 2020 The Authors. Published by IASE. This is an open access article under the CC BY-NC-ND license (<http://creativecommons.org/licenses/by-nc-nd/4.0/>).

1. Introduction

In our daily lives, most cosmic events in science, physics, and geometry are phenomena represented by nonlinear equations. Therefore, because of these nonlinearities, it is more difficult to solve these equations. Some of these nonlinear equations can be solved using approximate mathematical analytical methods such as the Homotopy (HAM) analysis method proposed by Liao (1992, 2004), the Homotopy Perturbation (HPM) method discovered by the mathematical scientist He (1999) and Adomain decomposition method (ADM) (Esmaili et al., 2008; Makinde and Mhone, 2006; Makinde, 2008). Some of these equations can be solved by conventional numerical methods such as finite difference method, the Keller box method, and Runge-Kutta methods. Recently some studies have shown a new method called the successive

linearization method (SLM). This method has been successfully applied to many non-linear problems in science and engineering, such as MHD flows of non-Newtonian fluids and transfer over a stretching sheet (Shateyi and Motsa, 2010), and the viscous pressure-flow between two parallel plates (Makukula et al., 2010a), a two-dimensional plate flowing between two porous walls (Makukula et al., 2010b), on the thin-film flow of Eyring-Powell fluid on the vertically moving belt (Salah et al., 2019) and convective thermal transfer heat to the MHD boundary layer with a pressure gradient (Ahmed et al., 2015). Therefore, this method has shown very high efficiency, accuracy, and flexibility of SLM in solving nonlinear equations.

In recent decades, the applications of liquids have become of great interest as they enter into many industrial products. Mathematically, however, some of these fluids are not easily expressed by a specific mathematical relationship between shear and stress rates, which are quite different from viscous fluids (Ellahi et al., 2008; Hayat et al., 2004). Examples of these fluids are very many and often found in homes, such as: Toiletries, paints, cosmetics, certain oils, shampoo, jam, soup, etc., have different characteristics and symbolize non-Newtonian fluids. In general, classification of non-Newtonian fluid

* Corresponding Author.

Email Address: frashed@kau.edu.sa<https://doi.org/10.21833/ijaas.2020.06.006>

Corresponding author's ORCID profile:

<https://orcid.org/0000-0003-0410-001X>

2313-626X/© 2020 The Authors. Published by IASE.

This is an open access article under the CC BY-NC-ND license

(<http://creativecommons.org/licenses/by-nc-nd/4.0/>)

models is given under three categories called integral, differential, and rate types (Fetecau et al., 2007; Salah et al., 2011; Hayat et al., 2008; Cortell, 2006). In this research, our main concern is to discuss the heat transfer flow of the magnetohydrodynamic (MHD) Oldroyd-B fluid overstretching. This application has attracted the attention of many scientists, and therefore conducted a large number of researches. The MHD fluid flow study can be carried out on the expansion plate for extrusion and drawing casting, plastic film, polymer, hot rolling, and many engineering applications. Following developments in this field, researchers in this field always try to improve accuracy using different methods of fluid behaviour. One of these methods used in this area is the application of dynamic magnetic flux (Ghadikolaei et al., 2018). This application is known as MHD. MHD is the study of the interaction of electrically conductive fluids with electromagnetic phenomena. Therefore, the flow of MHD liquid in the presence of a magnetic field is very, very important in many applications in science, engineering, and applied technology such as MHD pumps and nuclear power generation. Given these facts, many and many researchers continue to contribute to the field of MHD fluid mechanics (Hayat et al., 2013; Malik et al., 2013; Hussain et al., 2010; Husain et al., 2008). Another important application of nanoparticles in the base fluid, which seeks to improve the behaviour of fluids and recruitment, is the optimal use of changes. Because there are many different engineering issues and boundary conditions, extensive research has been conducted in this area, which is briefly summarized. Due to different boundary conditions and different geometric positions, Waqas et al. (2017) discussed the stratification of the nonliquid flow with generating heat in a stretchable linear surface. Ghadikolaei et al. (2018) analyzed the flow and heat of the second row liquid on a dilation sheet channel. The study of heat transfer with a mixed thermal flow of nonliquid that passes through a vertical plate extending with the presence of three different types of nanoparticles, Cu, Al₂O₃ and TiO₂ for the analysis of the different thermal conductivity of nonliquid and the speed of nanoparticles and research Nusselt number was found in Si et al. (2017). The works available in this introduction are listed in the references (Zargartalebi et al., 2015; Megahed, 2013; Sadeghy et al., 2006; Mukhopadhyay, 2012; Abel et al., 2012; Waqas et al., 2018; 2019a; Khan et al., 2019a; 2019b; Khan and Shehzad, 2019). The mixed convection flow resulting from forced and free convection contains many important practical applications in various industrial fields such as furnaces, astrophysics, geology, drying techniques, chemical treatments, etc. Forced convection is the temperature difference between the infinite thermal expansion disk resulting from free thermal flow and the heat transfer in the thermal expansion disc caused by the application of external forces. The mathematical model of buoyancy-driven flows becomes very complicated, resulting in the coupling

of thermal fields and transport properties of flows. A dimensionless parameter, namely Archimedes number $\frac{Gr}{Re^2}$ in mixed convection flow which represents distribution and comparative of natural convection to forced convection, play a critical and important role. For $\frac{Gr}{Re^2} > 1$, the free convection becomes governing over forced convection (Hashmi et al., 2017; Waqas et al., 2019b; Khan et al., 2018). At present, a new investigation is underway on the thermal transfer of the non-compressible Oldroyd-B liquid on an extended plate channel. The governing equations for the Oldroyd-B liquid are used with MHD. The numerical solution to the resulting nonlinear problem is calculated by using an SLM method. Embedded flow parameters are discussed and illustrated via diagrams.

2. Mathematical formulation of the problem

2.1. Flow analysis

Here we considering the two-dimensional steady laminar flow of an incompressible MHD Oldroyd-B fluid, which is past a flat sheet coincide with the plane $y = 0$, confining the flow to $y > 0$. Along x -axis, there are two opposite, and equal forces are applied. Due to this, the wall is stretched and reserving the origin fixed. Under the constant and boundary layer assumptions, the continuity, constitutive equation of Oldroyd-B fluid (Waqas et al., 2018) and energy equation (Cortell, 2006; Ghadikolaei et al., 2018) are:

$$\frac{\partial u}{\partial x} + \frac{\partial v}{\partial y} = 0, \quad (1)$$

$$u \frac{\partial u}{\partial x} + v \frac{\partial v}{\partial y} + \beta \left(u^2 \frac{\partial^2 u}{\partial x^2} + v^2 \frac{\partial^2 u}{\partial y^2} + 2uv \frac{\partial^2 u}{\partial x \partial y} \right) = v \left[\frac{\partial^2 u}{\partial y^2} + \gamma \left(u \frac{\partial^3 u}{\partial x \partial y^2} + v \frac{\partial^3 u}{\partial y^3} - \frac{\partial u}{\partial x} \frac{\partial^2 u}{\partial y^2} - \frac{\partial u}{\partial y} \frac{\partial^2 v}{\partial y^2} \right) \right] - \frac{\sigma B_0^2}{\rho} \left(u + \beta v \frac{\partial u}{\partial y} \right) + g \beta_T (T - T_\infty), \quad (2)$$

$$u \frac{\partial T}{\partial x} + v \frac{\partial T}{\partial y} = \alpha \frac{\partial^2 T}{\partial y^2} + \frac{v}{c_p} \left(\frac{\partial u}{\partial y} \right)^2, \quad (3)$$

where, (u, v) are the components of velocity in (x, y) directions, $\nu \left(= \frac{\mu}{\rho} \right)$ is the kinematic viscosity, μ is the dynamic viscosity, β is the relaxation time, γ is the retardation time, ρ is density of fluid, σ is the electric conductivity, B_0 is the uniform magnetic field, g is the gravitational acceleration, β_T is the coefficient of thermal expansion, T is temperature of fluid, $\alpha \left(= \frac{k}{\rho c} \right)$ is the thermal diffusivity, k the fluid thermal conductivity, ρc the fluid capacity heat and c_p is the specific heat of a fluid at constant pressure.

The relevant boundary conditions are defined as:

$$u = u_w = cx, \quad v = 0 \quad \text{at} \quad y = 0, \quad c > 0, \quad (4)$$

$$u \rightarrow 0, \quad \frac{\partial u}{\partial y} \rightarrow 0 \quad \text{as} \quad y \rightarrow \infty, \quad (5)$$

$$T = T_w (= T_\infty + Ax^s) \quad \text{at} \quad y = 0, \quad T \rightarrow T_\infty \quad \text{as} \quad y \rightarrow \infty, \quad (6)$$

where, c is the rate of stretching, T_w , T_∞ are constants, and s is the parameter wall temperature.

2.2. Transformation

Introducing the following dimensionless variables (Cortell, 2006; Ghadikolaie et al., 2018),

$$u = cx f'(\eta), \quad v = -(cv)^{\frac{1}{2}} f(\eta), \quad \eta = \left(\frac{c}{v}\right)^{\frac{1}{2}}, \quad \theta(\eta) = \frac{T - T_{\infty}}{T_w - T_{\infty}} \quad \text{and} \quad Ec = \frac{c^2}{Ap c}. \quad (7)$$

Utilizing Eq. 7, Eq. 1 is satisfied automatically and Eqs. 2 and 3 characterize to the following problems statement,

$$\begin{aligned} f''' + f f'' - f'^2 + \beta_1 (2 f f' f'' - f^2 f''') + \beta_2 (2 f f'' - f'^2 - f f^{iv}) - M^2 f' + \lambda \theta &= 0, \\ \theta'' + Pr f \theta' - s Pr f' \theta &= -Pr Ec (f'')^2 x^{2-s}. \end{aligned} \quad (8) \quad (9)$$

It is clear from Eq. 9 that all solutions are then of a similar type. If $s = 2$, and the effect of dissipative heat is neglected (Cortell, 2006), then we obtain the simpler equation from Eq. 9:

$$\theta'' + Pr f \theta' - s Pr f' \theta = 0, \quad (10)$$

here, $\beta_1 (= \beta c)$ is Deborah number in terms of relaxation time while $\beta_2 (= \gamma c)$ is Deborah number in terms of retardation time, $M (= \sqrt{\sigma B_0^2 / c \rho})$ is the Hartman number, $\lambda (= \frac{Gr_x}{Re_x^2})$ is the mixed convection parameter, $Pr (= \frac{\nu}{\alpha})$ is the Prandtl number and $E (= \frac{c^2}{Ap c})$ is the Eckert number.

The related boundary conditions:

$$f = 0, f' = 1 \quad \text{at} \quad \eta = 0, \quad (11)$$

$$f' \rightarrow 0, f'' \rightarrow 0 \quad \text{as} \quad \eta \rightarrow \infty, \quad (12)$$

$$\theta(0) = 1, \quad \theta(\infty) \rightarrow 0. \quad (13)$$

3. Solution the problem

3.1. Procedure of computational

Here successive linearization method (SLM) (Makukula et al., 2020b; Salah et al., 2019; Ahmed et al., 2015) is implemented to obtain the numerical solutions for nonlinear systems in Eqs. 8 and 10 corresponding to the boundary condition in Eqs. 11-13.

For SLM solution we select the initial guesses functions $f(\eta)$ and $\theta(\eta)$ in the form,

$$f(\eta) = f_i(\eta) + \sum_{m=0}^{i-1} F_m(\eta), \quad \theta(\eta) = \theta_i(\eta) + \sum_{m=0}^{i-1} \theta_m(\eta), \quad (14)$$

here, the two functions $f_i(\eta)$ and $\theta_i(\eta)$ are representative of unknown functions. $F_m(\eta), m \geq 1, \theta_m(\eta), m \geq 1$ are a successive approximation, which are obtained by recursively solving the linear part of the equation that results from substituting Eq. 14 in the governing equations. The mean idea of SLM that the assumption of unknown function $f_i(\eta)$ and $\theta_i(\eta)$ are very small when i becomes larger,

therefore, the nonlinear terms in $f_i(\eta), \theta_i(\eta)$ and their derivatives are considered to be smaller and thus neglected. The intimal guess functions $F_0(\eta), \theta_0(\eta)$ which are selected to satisfy the boundary conditions,

$$\begin{aligned} F_0(\eta) &= 0, \quad F'_0(\eta) = 1 \quad \text{at} \quad \eta = 0, \\ F'_0(\eta) &\rightarrow 0, F''_0(\eta) \rightarrow 0 \quad \text{at} \quad \eta \rightarrow \infty, \\ \theta_0(0) &= 1, \quad \theta_0(\infty) \rightarrow 0. \end{aligned} \quad (15)$$

which are taken to be in the form,

$$F_0(\eta) = (1 - e^{-\eta}) \quad \text{and} \quad \theta_0(\eta) = e^{-\eta}. \quad (16)$$

Therefore, beginning from the initial guess, the subsequent solution F_i and θ_i are calculated by successively solving the linearized from the equation, which is obtained by substituting Eq. 14 in the governing Eqs. 8 and 10. Then we arrive at the linearized equations to be solved are:

$$\begin{aligned} a_{1,i-1} F_i^{iv} + a_{2,i-1} F_i''' + a_{3,i-1} F_i'' + a_{4,i-1} F_i' + a_{5,i-1} F_i + \\ \lambda \theta_i = r_{1,i-1}, \end{aligned} \quad (17)$$

$$b_{1,i-1} F_i' + b_{2,i-1} F_i + \theta_i'' + b_{3,i-1} \theta_i' + b_{4,i-1} \theta_i = r_{2,i-1}. \quad (18)$$

Subject to the boundary conditions,

$$F_i(0) = \theta_i(\infty) = 0, \quad F'_i(0) = \theta_i(0) = 1, \quad (19)$$

where, the coefficients parameters $a_{k,i-1}, b_{h,i-1} (k = 1, 2, 3, 4, 5), (h = 1, 2, 3, 4)$ and $r_{j,i-1}, j = 1, 2$ are defined as,

$$\begin{aligned} a_{2,i-1} &= 1 - \beta_1 \left(\sum_{m=0}^{i-1} F_m \right)^2 + 2\beta_2 \sum_{m=0}^{i-1} F_m', \\ a_{3,i-1} &= \sum_{m=0}^{i-1} F_m + 2\beta_1 \sum_{m=0}^{i-1} F_m \sum_{m=0}^{i-1} F_m' - \\ &2\beta_2 \sum_{m=0}^{i-1} F_m'', \\ a_{4,i-1} &= -2 \sum_{m=0}^{i-1} F_m' - M^2 + 2\beta_1 \sum_{m=0}^{i-1} F_m \sum_{m=0}^{i-1} F_m'' + \\ &2\beta_2 \sum_{m=0}^{i-1} F_m''', \\ a_{5,i-1} &= \sum_{m=0}^{i-1} F_m'' + 2\beta_1 \sum_{m=0}^{i-1} F_m \sum_{m=0}^{i-1} F_m'' - \\ &2\beta_1 \sum_{m=0}^{i-1} F_m \sum_{m=0}^{i-1} F_m''' - \beta_2 \sum_{m=0}^{i-1} F_m^{iv}, \end{aligned}$$

and,

$$\begin{aligned} r_{1,i-1} &= - \sum_{m=0}^{i-1} F_m''' - \sum_{m=0}^{i-1} F_m \sum_{m=0}^{i-1} F_m'' + \\ &\left(\sum_{m=0}^{i-1} F_m' \right)^2 - \beta_1 \left[2 \sum_{m=0}^{i-1} F_m \sum_{m=0}^{i-1} F_m' \sum_{m=0}^{i-1} F_m'' - \right. \\ &\left. \left(\sum_{m=0}^{i-1} F_m \right)^2 \sum_{m=0}^{i-1} F_m''' \right] - \beta_2 \left[2 \sum_{m=0}^{i-1} F_m \sum_{m=0}^{i-1} F_m'' - \right. \\ &\left. \left(\sum_{m=0}^{i-1} F_m' \right)^2 - \sum_{m=0}^{i-1} F_m \sum_{m=0}^{i-1} F_m^{iv} \right] + M^2 \sum_{m=0}^{i-1} F_m' - \\ &\lambda \sum_{m=0}^{i-1} \theta_m, \\ -2Pr \sum_{m=0}^{i-1} \theta_m, \quad b_{2,i-1} &= Pr \sum_{m=0}^{i-1} \theta_m', \quad b_{3,i-1} = Pr \sum_{m=0}^{i-1} F_m, \end{aligned} \quad (20)$$

$$\begin{aligned} b_{4,i-1} &= -2Pr \sum_{m=0}^{i-1} F_m', \\ r_{2,i-1} &= - \sum_{m=0}^{i-1} \theta_m'' - Pr \sum_{m=0}^{i-1} F_m \sum_{m=0}^{i-1} \theta_m' + \\ Pr \sum_{m=0}^{i-1} F_m' \sum_{m=0}^{i-1} \theta_m. \end{aligned} \quad (21)$$

When we solve Eqs. 8 and 10 iteratively, the solution for F_i and θ_i has been obtained and finally after K iterations the solution $f(\eta)$ and $\theta(\eta)$ can be written as $f(\eta) \approx \sum_{m=0}^K F_m(\eta), \theta(\eta) \approx \sum_{m=0}^K \theta_m(\eta)$.

In order to apply SLM, firstly, transform the domain solution from $[0, \infty)$ to $[-1, 1]$. SLM is based on the Chebyshev spectral collection method. This method is depending on the Chebyshev polynomials defined on the interval $[-1, 1]$. Thus, by using the truncation of the domain approach where the problem is solved in the interval $[0, L]$, where L is a scaling parameter used to impose the boundary condition at infinity. Thus, this can be obtained via the transformation,

$$\frac{\eta}{L} = \frac{\xi+1}{2}, \quad -1 \leq \xi \leq 1. \quad (22)$$

By using the Gauss-Lobatto collocation points, we can discretize the domain $[-1, 1]$ as follows:

$$\xi = \cos \frac{\pi j}{N}, \quad F_i \approx \sum_{k=0}^N F_i(\xi_k) T(\xi_j), \quad j = 0, 1, \dots, N, \quad (23)$$

where, N is the number of collection points and T_k is the k^{th} Chebyshev polynomial given by $T_k(\xi) = \cos[k \cos^{-1}(\xi)]$.

The derivatives of the variable at the collocation points are in the form,

$$\begin{aligned} \frac{d^r F_i}{d\eta^r} &= \sum_{k=0}^N \mathbf{D}_{kj}^r F_i(\xi_k), \quad j = 0, 1, \dots, N, \\ \frac{d^r \theta_i}{d\eta^r} &= \sum_{k=0}^N \mathbf{D}_{kj}^r \theta_i(\xi_k), \quad j = 0, 1, \dots, N, \end{aligned} \quad (24)$$

where r is the order of differentiation and $\mathbf{D} = \frac{2}{L} D$ with D is the Chebyshev spectral differentiation matrix. Substituting Eqs. 22 to 24 into Eqs. 17 and 18 we arrive at the matrix equation:

$$\mathbf{A}_{i-1} \mathbf{X}_i = \mathbf{R}_{i-1}, \quad (25)$$

where,

$$\begin{aligned} \mathbf{A}_{i-1} &= \begin{bmatrix} \mathbf{A}_{11} & \mathbf{A}_{12} \\ \mathbf{A}_{21} & \mathbf{A}_{22} \end{bmatrix}, \quad \mathbf{X}_{i-1} = \begin{bmatrix} F_i \\ \theta_i \end{bmatrix}, \quad \mathbf{R}_{i-1} = \begin{bmatrix} r_{1,i-1} \\ r_{2,i-1} \end{bmatrix}, \\ \mathbf{A}_{11} &= a_{1,i-1} \mathbf{D}^4 + a_{2,i-1} \mathbf{D}^3 + a_{3,i-1} \mathbf{D}^2 + a_{4,i-1} \mathbf{D} + a_{5,i-1} \mathbf{I}, \\ \mathbf{A}_{12} &= \lambda \mathbf{I}, \\ \mathbf{A}_{21} &= b_{1,i-1} \mathbf{D} + b_{2,i-1} \mathbf{I}, \\ \mathbf{A}_{22} &= \mathbf{D}^2 + b_{3,i-1} \mathbf{D} + b_{4,i-1} \mathbf{I}. \end{aligned} \quad (26)$$

Following the above procedure, we can obtain the solution as $\mathbf{X}_i = \mathbf{A}_{i-1}^{-1} \mathbf{R}_{i-1}$

3.2. Convergence analysis

The convergence for numerical values of $-f''(0)$ for different order of approximation when $M = 0.50, \beta_1 = 0.20, \beta_2 = 0.01, Pr = 1.00$ and $\lambda = 0.20$ is shown in Table 1.

3.3. Numerical scheme testing

The aim here is to test our numerical results and compare them with published works results in the literature as limiting cases situations. Thus, we compare the present results with the available results in reference (Cortell, 2006; Ghadikolaei et al., 2018; Waqas et al., 2017; Megahed, 2013; Sadeghy et al., 2006; Mukhopadhyay, 2012). It is found that our

results are in excellent agreement with those of Cortell (2006), Ghadikolaei et al. (2018), Waqas et al. (2017), Megahed (2013), Sadeghy et al. (2006), and Mukhopadhyay (2012) as shown in Tables 2-5.

Table 1: The convergence for numerical values of $-f''(0)$ for different order of approximation when, $M = 0.50, \beta_1 = 0.20, \beta_2 = 0.01, Pr = 1.00$ and $\lambda = 0.20$

Order of approximation	$-f''(0)$	$-\theta'(0)$
1	1.0145745392	1.3289761386
5	1.0458522661	1.3178799143
10	1.0625824893	1.3109508206
20	1.0721659565	1.3070530958
30	1.0735888962	1.3065067051
50	1.0737954104	1.3064333815
70	1.0737972453	1.3064330292
100	1.0737971920	1.3064330634
105	1.0737971915	1.3064330637
110	1.0737971913	1.3064330638
120	1.0737971911	1.3064330639
130	1.0737971911	1.3064330639
140	1.0737971911	1.3064330639
150	1.0737971911	1.3064330639

Table 2: Comparison of numerical values of $-f''(0)$ with references Waqas et al. (2017) and Megahed (2013) for several values of β_1 when, $M = \beta_2 = Pr = \lambda = 0.00$

β_1	Megahed (2013)	Waqas et al. (2017)	Present work
0.0	0.999978	1.000000	0.999999
0.2	1.051945	1.051889	1.051889
0.4	1.101848	1.101903	1.101903
0.6	1.150163	1.150137	1.150137
0.8	1.196690	1.196711	1.196711
1.0	-	-	1.241747

Table 3: Comparative analysis of numerical values of $-f''(0)$ with References Sadeghy et al. (2006) and Mukhopadhyay (2012) for several values of β_1 when, $M = \beta_2 = Pr = \lambda = 0.00$

β_1	Sadeghy et al. (2006)	Mukhopadhyay (2012)	Present work
0.0	1.000000	0.9999963	0.999999
0.2	1.05194	1.051949	1.051889
0.4	1.10084	1.101851	1.101903
0.6	1.0015016	1.150162	1.150137
0.8	1.19872	1.196693	1.196711
1.0	-	-	1.241747

Table 4: Comparison of numerical values of $f(\eta)$ with Ghadikolaei et al. (2018) when, $M = \beta_1 = Pr = \lambda = 0.00$ and $\beta_2 = 0.01$

β_2	η	Ghadikolaei et al. (2018)	Present work
0.01	0	0	0
	0.1	0.095199	0.095194
	0.2	0.181400	0.181338
	0.5	0.394050	0.393892
	1	0.633463	0.633460
	2	0.866679	0.867642
	3	0.952228	0.954211
	4	0.983566	0.986229
	5	-	0.998059

4. Results and discussion

In this section, we present the graphs obtained using the successive linear method of speed and temperature profiles. These drawings show differences in the flow parameters included in the solution expressions for the heat transfer analysis of the non-compressible MHD flow of Oldroyd-B liquid on an extended plate channel. Physical explanations

and the behavioural parameters of the problem are discussed in Fig. 1 to Fig. 10.

Table 5: Comparison of numerical values of $-\theta'(0)$ with Cortell (2006) when, $M = \beta_1 = Pr = \lambda = 0.00$ and $\beta_2 = 0.01$

β_2	η	Cortell (2006)	Present work
0.01	0	1.334735	1.334733
	0.1	1.150410	1.150382
	0.2	0.993973	0.994026
	0.5	0.650461	0.650523
	1	0.335684	0.335643
	2	0.102150	0.102133
	3	-	0.034583
	4	-	0.012274
	5	0.004444	0.004441
	10	2×10^{-5}	0.000029

These figures are drawn to illustrate these differences. Here the flow diagrams of the MHD heat transfer flow of the Oldroyd-B fluid fixed on the expansion board are determined. In Fig. 1 we can see the effects of the applied magnetic field (Hartmann's number) M on the velocity profile. By maintaining β_1, Pr, λ its stability and contrast M , it turns out that the velocity profile decreases when the magnetic field parameter M becomes larger. From the physical side, we notice that when we increase its value, the flow on the profile $f'(\eta)$ of speed decreases, in fact due to the effect of the transverse magnetic field on the electrically conductive fluid, which produces a Lorentz-type resistance force that tends to slow the movement of the fluid and limits its movement and speed. Fig. 2 shows that for the strong magnetic force imposed, this leads to a large temperature, and this is due to the fact that in the strong magnetic foreground, Lorenz's force becomes dominant, and then the result increases the temperature of the liquid. Fig. 3 illustrates the effects of the mixed convection parameter λ on the velocity profile when β_1, Pr, M are constant. It should be noted that by increasing the λ parameter, buoyancy increases due to increased gravity and as a result increases speed. Besides, the thickness of the large λ border layer is also increasing. In Fig. 4, we illustrate that for a larger size of λ , this may lead to an increase in coil temperature (this is very much related to the decrease in the thickness of the boundary layer). Fig. 5 is plotted for the Prandtl number Pr variance $\theta(\eta)$. Note that for a large Pr , the thermal field is lower and then reduces the temperature. In fact, the Prandtl number assists liquids in higher thermal conductivity and this creates a thicker thermal boundary layer of large. It is noted that from Fig. 6, Prandtl number Pr has the same effect on the same temperature. The effect of the Deborah number β_1 on the velocity distribution $f'(\eta)$ is shown by Fig. 7 and Fig. 8. In fact, comes mainly because of the relaxation time phenomena. A lot leads to a longer relaxation time that interferes with the flow of liquid, and then the thickness of the momentum layer is reduced. Fig. 8 illustrates the effect of β_1 on temperature profile over the sheet, and we note that by increasing in β_1 parameter is seen to decrease and reducing in the liquid temperature $\theta(\eta)$.

Physically, that is, for the larger parameter, the thermal border layer becomes thicker. Finally, Fig. 9 and Fig. 10 show an effect of β_2 on the velocity and temperature profiles on the paper, and note that by increasing the parameter β_2 the effect is seen to be very small for both features. Moreover, the second grade, Maxwell and viscous cases are retrieved by setting $\beta_1 = 0$, $\beta_2 = 0$, and $\beta_1 = \beta_2 = 0$.

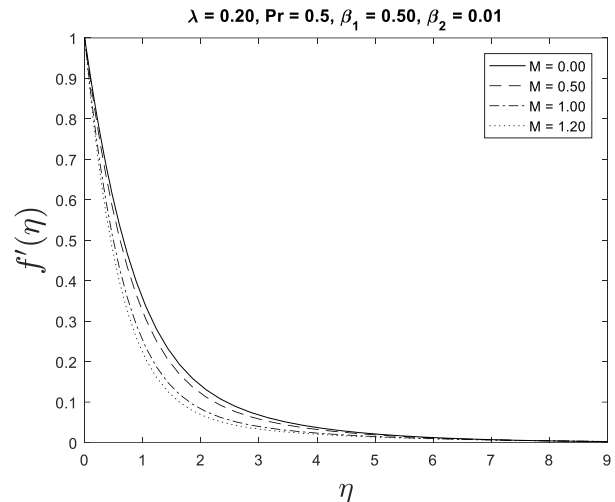


Fig. 1: Effects of Hartman number M for $f'(\eta)$

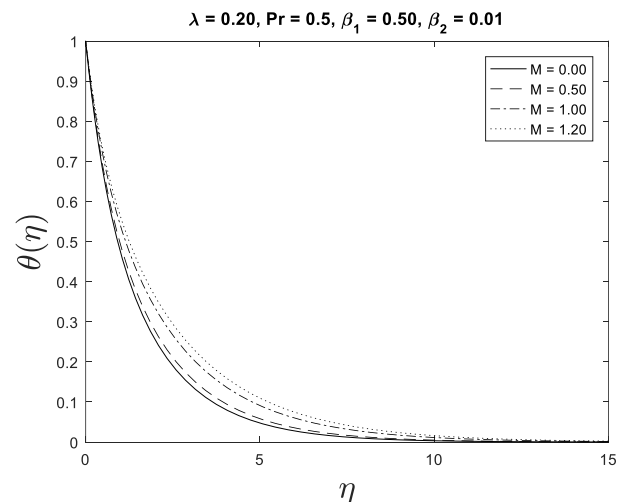


Fig. 2: Effects of Hartman number M for $\theta(\eta)$

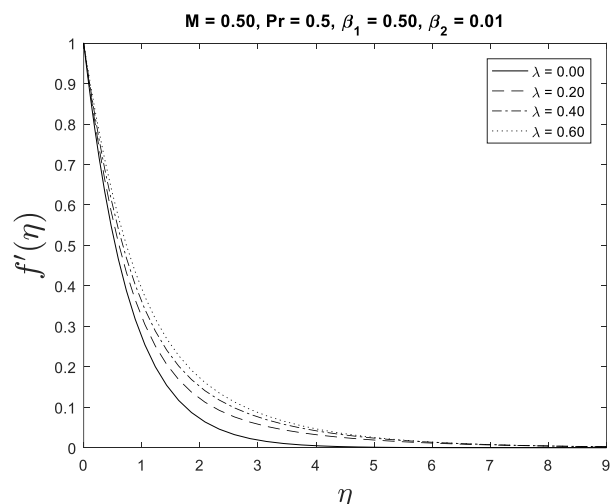


Fig. 3: Effects of mixed convection parameter λ for $f'(\eta)$

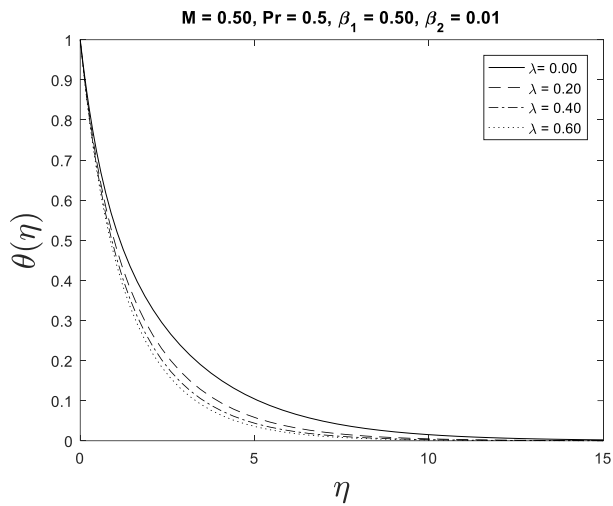


Fig. 4: Effects of mixed convection parameter λ for $\theta(\eta)$

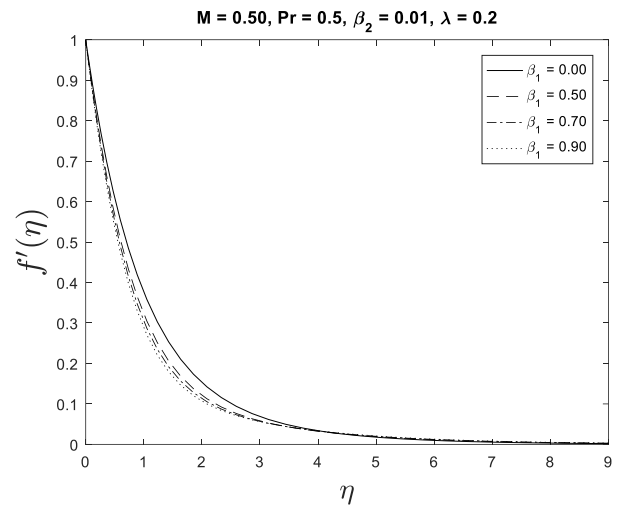


Fig. 7: Effects of Deborah number β_1 for $f'(\eta)$

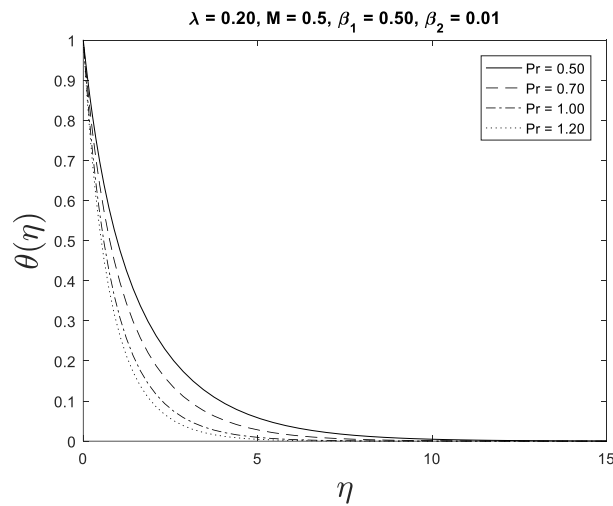


Fig. 5: Effects of Prandtl number Pr for $\theta(\eta)$

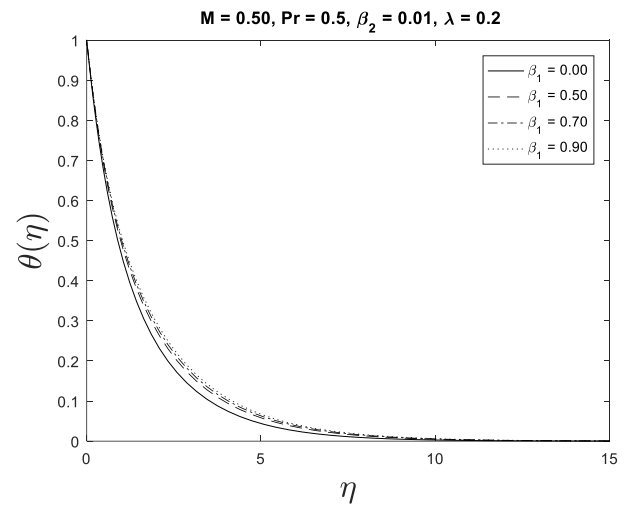


Fig. 8: Effects of Deborah number β_1 for $\theta(\eta)$

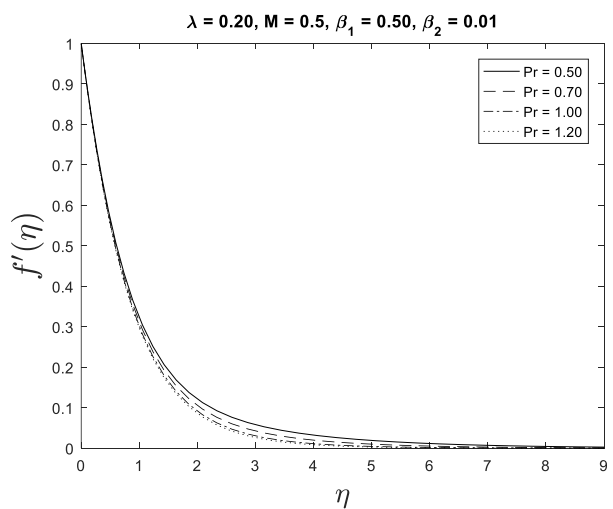


Fig. 6: Effects of Prandtl number Pr for $f'(\eta)$

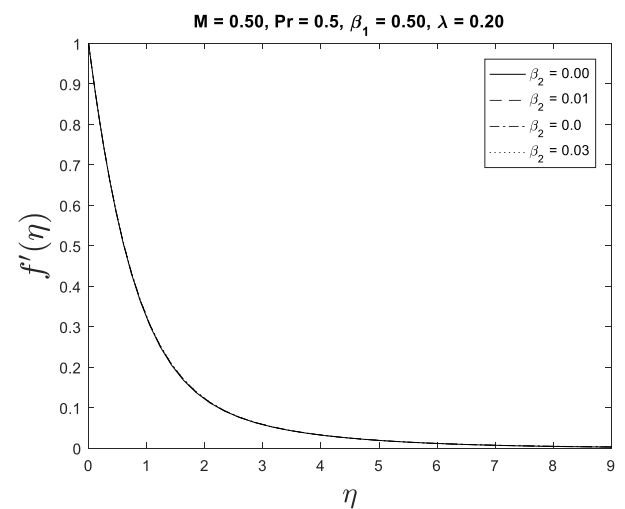


Fig. 9: Effects of Deborah number β_2 for $f'(\eta)$

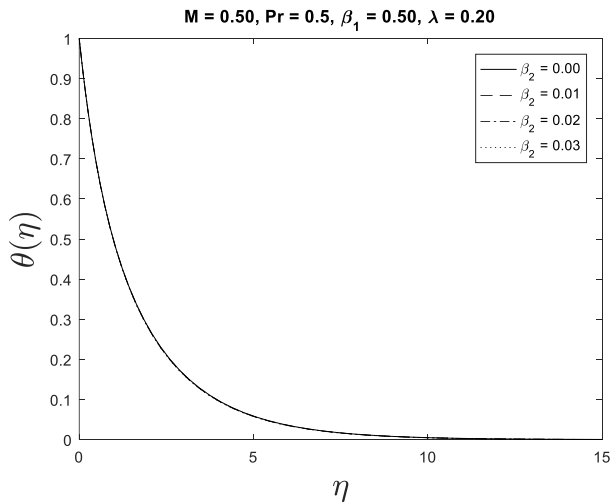


Fig. 10: Effects of Deborah number β_2 for $\theta(\eta)$

5. Conclusion

In this research, the problem of MHD heat transfer of an incompressible Oldroyd-B fluid on a stretching sheet channel is solved numerically. The numerical solutions are well established by SLM. The influence of various parameters is shown through different graphs. The present results have been tested and compared with the available published results in Cortell (2006), Ghadikolaei et al. (2018) and Waqas et al. (2017), Megahed (2013), Sadeghy et al. (2006) and Mukhopadhyay (2012) in a limiting situation shown in Tables 2-5 and an excellent agreement is found.

Compliance with ethical standards

Conflict of interest

The authors declare that they have no conflict of interest.

References

- Abel MS, Tawade JV, and Nandeppanavar MM (2012). MHD flow and heat transfer for the upper-convected Maxwell fluid over a stretching sheet. *Meccanica*, 47(2): 385-393. <https://doi.org/10.1007/s11012-011-9448-7>
- Ahmed MAM, Mohammed ME, and Khidir AA (2015). On linearization method to MHD boundary layer convective heat transfer with low pressure gradient. *Propulsion and Power Research*, 4(2): 105-113. <https://doi.org/10.1016/j.jprr.2015.04.001>
- Cortell R (2006). A note on flow and heat transfer of a viscoelastic fluid over a stretching sheet. *International Journal of Non-Linear Mechanics*, 41(1): 78-85. <https://doi.org/10.1016/j.ijnonlinmec.2005.04.008>
- Ellahi R, Hayat T, Javed T, and Asghar S (2008). On the analytic solution of nonlinear flow problem involving Oldroyd 8-constant fluid. *Mathematical and Computer Modelling*, 48(7-8): 1191-1200. <https://doi.org/10.1016/j.mcm.2007.12.017>
- Esmaili Q, Ramiar A, Alizadeh E, and Ganji DD (2008). An approximation of the analytical solution of the Jeffery-Hamel flow by decomposition method. *Physics Letters A*, 372(19): 3434-3439. <https://doi.org/10.1016/j.physleta.2008.02.006>
- Fetecau C, Prasad SC, and Rajagopal KR (2007). A note on the flow induced by a constantly accelerating plate in an Oldroyd-B fluid. *Applied Mathematical Modelling*, 31(4): 647-654. <https://doi.org/10.1016/j.apm.2005.11.032>
- Ghadikolaei SS, Hosseinzadeh K, Yassari M, Sadeghi H, and Ganji DD (2018). Analytical and numerical solution of non-Newtonian second-grade fluid flow on a stretching sheet. *Thermal Science and Engineering Progress*, 5: 309-316. <https://doi.org/10.1016/j.tsep.2017.12.010>
- Hashmi MS, Khan N, Khan SU, and Rashidi MM (2017). A mathematical model for mixed convective flow of chemically reactive Oldroyd-B fluid between isothermal stretching disks. *Results in Physics*, 7: 3016-3023. <https://doi.org/10.1016/j.rinp.2017.08.017>
- Hayat T, Awais M, and Asghar S (2013). Radiative effects in a three-dimensional flow of MHD Eyring-Powell fluid. *Journal of the Egyptian Mathematical Society*, 21(3): 379-384. <https://doi.org/10.1016/j.joems.2013.02.009>
- Hayat T, Fetecau C, and Sajid M (2008). Analytic solution for MHD transient rotating flow of a second grade fluid in a porous space. *Nonlinear Analysis: Real World Applications*, 9(4): 1619-1627. <https://doi.org/10.1016/j.nonrwa.2007.04.006>
- Hayat T, Khan M, and Ayub M (2004). Couette and Poiseuille flows of an Oldroyd 6-constant fluid with magnetic field. *Journal of Mathematical Analysis and Applications*, 298(1): 225-244. <https://doi.org/10.1016/j.jmaa.2004.05.011>
- He JH (1999). Homotopy perturbation technique. *Computer Methods in Applied Mechanics and Engineering*, 178(3-4): 257-262. [https://doi.org/10.1016/S0045-7825\(99\)00018-3](https://doi.org/10.1016/S0045-7825(99)00018-3)
- Husain M, Hayat T, Fetecau C, and Asghar S (2008). On accelerated flows of an Oldroyd-B fluid in a porous medium. *Nonlinear Analysis: Real World Applications*, 9(4): 1394-1408. <https://doi.org/10.1016/j.nonrwa.2007.03.007>
- Hussain M, Hayat T, Asghar S, and Fetecau C (2010). Oscillatory flows of second grade fluid in a porous space. *Nonlinear Analysis: Real World Applications*, 11(4): 2403-2414. <https://doi.org/10.1016/j.nonrwa.2009.07.016>
- Khan SU and Shehzad SA (2019). Brownian movement and thermophoretic aspects in third-grade nanofluid over oscillatory moving sheet. *Physica Scripta*, 94: 9. <https://doi.org/10.1088/1402-4896/ab0661>
- Khan SU, Rauf A, Shehzad SA, Abbas Z, and Javed T (2019a). Study of bioconvection flow in Oldroyd-B nanofluid with motile organisms and effective Prandtl approach. *Physica A: Statistical Mechanics and its Applications*, 527: 121179. <https://doi.org/10.1016/j.physa.2019.121179>
- Khan SU, Shehzad SA, and Ali N (2018). Interaction of magneto-nanoparticles in Williamson fluid flow over convective oscillatory moving surface. *Journal of the Brazilian Society of Mechanical Sciences and Engineering*, 40: 195. <https://doi.org/10.1007/s40430-018-1126-4>
- Khan SU, Shehzad SA, and Nasir S (2019b). Unsteady flow of chemically reactive Oldroyd-B fluid over oscillatory moving surface with thermo-diffusion and heat absorption/generation effects. *Journal of the Brazilian Society of Mechanical Sciences and Engineering*, 41: 72. <https://doi.org/10.1007/s40430-019-1577-2>
- Liao S (2004). On the homotopy analysis method for nonlinear problems. *Applied Mathematics and Computation*, 147(2): 499-513. [https://doi.org/10.1016/S0096-3003\(02\)00790-7](https://doi.org/10.1016/S0096-3003(02)00790-7)
- Liao SJ (1992). The proposed homotopy analysis technique for the solution of nonlinear problems. Ph.D. Dissertation, Shanghai Jiao Tong University, Shanghai, China.
- Makeinde OD (2008). Effect of arbitrary magnetic Reynolds number on MHD flows in convergent-divergent channels. *International Journal of Numerical Methods for Heat and Fluid*

- Flow, 18(6): 697-707.
<https://doi.org/10.1108/09615530810885524>
- Makinde OD and Mhone PY (2006). Hermite–Padé approximation approach to MHD Jeffery–Hamel flows. *Applied Mathematics and Computation*, 181(2): 966-972.
<https://doi.org/10.1016/j.amc.2006.02.018>
- Makukula Z, Motsa SS, and Sibanda P (2010a). On a new solution for the viscoelastic squeezing flow between two parallel plates. *Journal of Advanced Research in Applied Mathematics*, 2(4): 31-38.
<https://doi.org/10.5373/jaram.455.060310>
- Makukula ZG, Sibanda P, and Motsa SS (2010b). A novel numerical technique for two-dimensional laminar flow between two moving porous walls. *Mathematical Problems in Engineering*, 2010: 528956.
<https://doi.org/10.1155/2010/528956>
- Malik MY, Hussain A, and Nadeem S (2013). Boundary layer flow of an Eyring–Powell model fluid due to a stretching cylinder with variable viscosity. *Scientia Iranica*, 20(2): 313-321.
<https://doi.org/10.1016/j.scient.2013.02.028>
- Megahed AM (2013). Variable fluid properties and variable heat flux effects on the flow and heat transfer in a non-Newtonian Maxwell fluid over an unsteady stretching sheet with slip velocity. *Chinese Physics B*, 22: 9.
<https://doi.org/10.1088/1674-1056/22/9/094701>
- Mukhopadhyay S (2012). Heat transfer analysis of the unsteady flow of a Maxwell fluid over a stretching surface in the presence of a heat source/sink. *Chinese Physics Letters*, 29: 5.
<https://doi.org/10.1088/0256-307X/29/5/054703>
- Sadeghy K, Hajibeygi H, and Taghavi SM (2006). Stagnation-point flow of upper-convected Maxwell fluids. *International Journal of Non-Linear Mechanics*, 41(10): 1242-1247.
<https://doi.org/10.1016/j.ijnonlinmec.2006.08.005>
- Salah F, Abdul Aziz Z, Ching C, and Ling D (2011). New exact solutions for MHD transient rotating flow of a second-grade fluid in a porous medium. *Journal of Applied Mathematics*, 2011: 823034.
<https://doi.org/10.1155/2011/823034>
- Salah F, Alzahrani AK, Sidahmed AO, and Viswanathan KK (2019). A note on thin-film flow of Eyring-Powell fluid on the vertically moving belt using successive linearization method. *International Journal of Advanced and Applied Sciences*, 6(2): 17-22.
<https://doi.org/10.21833/ijaas.2019.02.004>
- Shateyi S and Motsa SS (2010). Variable viscosity on magnetohydrodynamic fluid flow and heat transfer over an unsteady stretching surface with Hall effect. *Boundary Value Problems*, 2010(1): 257568.
<https://doi.org/10.1155/2010/257568>
- Si X, Li H, Zheng L, Shen Y, and Zhang X (2017). A mixed convection flow and heat transfer of pseudo-plastic power law nanofluids past a stretching vertical plate. *International Journal of Heat and Mass Transfer*, 105: 350-358.
<https://doi.org/10.1016/j.ijheatmasstransfer.2016.09.106>
- Waqas H, Imran M, Khan SU, Shehzad SA, and Meraj MA (2019b). Slip flow of Maxwell viscoelasticity-based micropolar nanoparticles with porous medium: A numerical study. *Applied Mathematics and Mechanics*, 40(9): 1255-1268.
<https://doi.org/10.1007/s10483-019-2518-9>
- Waqas H, Khan SU, Hassan M, Bhatti MM, and Imran M (2019a). Analysis on the bioconvection flow of modified second-grade nanofluid containing gyrotactic microorganisms and nanoparticles. *Journal of Molecular Liquids*, 291: 111231.
<https://doi.org/10.1016/j.molliq.2019.111231>
- Waqas M, Hayat T, Shehzad SA, and Alsaedi A (2018). Transport of magnetohydrodynamic nanomaterial in a stratified medium considering gyrotactic microorganisms. *Physica B: Condensed Matter*, 529: 33-40.
<https://doi.org/10.1016/j.physb.2017.09.128>
- Waqas M, Khan MI, Hayat T, and Alsaedi A (2017). Stratified flow of an Oldroyd-B nanoliquid with heat generation. *Results in Physics*, 7: 2489-2496.
<https://doi.org/10.1016/j.rinp.2017.06.030>
- Zargartalebi H, Ghalambaz M, Noghrehabadi A, and Chamkha A (2015). Stagnation-point heat transfer of nanofluids toward stretching sheets with variable thermo-physical properties. *Advanced Powder Technology*, 26(3): 819-829.
<https://doi.org/10.1016/j.appt.2015.02.008>